Research Article Vol. 2, No. 9 / September 2015 / Optica 803

Nonlinear absorbance in dielectric multilayers

O. Razskazovskaya,[1,†] T. T. Luu,[1,†] M. Trubetskov,[1,2] E. Goulielmakis,[1] and V. Pervak[3,4,*]

[1]Max-Planck Institute for Quantum Optics, Hans-Kopfermann-str. 1, D-85748 Garching, Germany
[2]Research Computer Center, Moscow State University, Leninskie Gory, 119992 Moscow, Russia
[3]Chair of Physics, Ludwig-Maximilian University Munich, Am Coulombwall 1, D-85748 Garching, Germany
[4]Ultrafast Innovations GmbH, Am Coulombwall 1, D-85748 Garching, Germany
*Corresponding author: vladimir.pervak@physik.uni-muenchen.de

Received 1 May 2015; revised 19 June 2015; accepted 7 July 2015 (Doc. ID 239903); published 11 September 2015

Within the last two decades dispersive dielectric multilayer mirrors (DMs), also known as chirped mirrors (CMs), have played a significant role in the progress of ultrafast science. Their ability to manipulate the phase of a light pulse has advanced the synthesis of intense femtosecond optical pulses followed by remarkable progress in the disciplines of nonlinear optics. Meanwhile, the performance of the mirrors themselves has been strictly limited to the linear regime, as essential mirror characteristics such as reflectance, transmittance, and dispersion are evaluated with only intensity-independent values of refractive indices and extinction coefficients taken into the design formalism. Here, we report, to the best of our knowledge, the first observation of a strong nonlinear response of the DMs. We have found that the DM's multilayer stack causes very significant enhancement of the internal electric field that becomes sufficient to enable third-order nonlinearity. Remarkably, in our particular case, the response is solely emerging in the form of nonlinear absorbance. By modifying the multilayer structure of the mirror, we gained control over observed nonlinearity and were able to predict and to some extent to tune the magnitude of the response, without perturbing the dispersive properties of the DMs. This demonstration not only expands the functionality of DMs into the nonlinear domain, but also marks a new approach to the development of multilayer coatings for applications in ultrafast science. © 2015 Optical Society of America

OCIS codes: (320.7110) Ultrafast nonlinear optics; (320.5520) Pulse compression; (310.1620) Interference coatings; (310.6860) Thin films, optical properties; (310.4165) Multilayer design; (310.6805) Theory and design.

http://dx.doi.org/10.1364/OPTICA.2.000803

1. INTRODUCTION

The vast progress of ultrafast optics has permitted the generation of light pulses confined to few-cycles of the oscillating electric and magnetic fields [1,2]. One of the key technologies empowering these few-cycle systems is the utilization of DMs [3–6]. The term dielectric multilayer mirror (DM) generally refers to a multilayer dielectric thin-film coating capable of introducing a chosen, engineered group delay (GD).

Due to the extreme temporal and spatial confinement of the generated few-cycle pulses, laser systems with moderate average powers yield pulse peak intensities on the target in the order of petawatts (10^{15} W), thus allowing us to enter the strong-field regime of nonlinear optics [7]. The ongoing development of broadband optical parametric amplifiers (OPAs) holds promise for further scaling of achievable peak intensities [8,9]. While experiment is exposed to the petawatt level intensities, the optics of the delivering systems is driven in the terawatt (10^{12} W) regime, a regime at which the response is dominated by low order bound electronic nonlinearities such as the second- and third-order processes, consequently making it a perturbative regime [7]. The appearance of nonlinearities in bulk components such as lenses and windows is well recognized and addressed in the literature; however, the performance of the thin-film coatings, and DMs in particular, has hitherto been considered in the linear domain only.

In this paper we report on the first observation, to the best of our knowledge, of a nonlinear response of the dielectric DMs. We have found that the complicated interference pattern within the DMs' multilayer stack causes a certain distribution of the electric field inside the coating that gives rise to a very significant enhancement of the internal electric field. It is known that multilayer structures such as Bragg reflectors or resonant cavities and quantum wells are capable of enhancing the nonlinear response [10–12]; however, even then the materials with relatively large nonlinear refractive indices, mostly semiconductors and polymers [13–16], are used in order to achieve reasonable scale of nonlinearity. In our case the enhancement becomes sufficient to trigger third-order nonlinear optical processes in the dielectric materials of the multilayer that have orders of magnitude smaller nonlinear coefficients than common semiconductors/polymers [17,18], which indicates the significance of the enhancement factor.

We have also found that in our case two-photon absorption (2PA) strongly dominates the observed nonlinearity, as the nonlinear response of the DMs emerges in the form of nonlinear

absorbance, while the appearance of the optical Kerr effect—second manifestation of third-order nonlinearity—is not evident.

Despite the fact that at first sight the observed nonlinearity appears to be unwanted only, as it impairs the performance of the ultrafast system, the authors see attractive and worthwhile applications, which will be discussed later.

Based on experimental data, we have developed a theoretical model that allows estimation of the coefficient of 2PA and consequently prediction and to some extent tuning of the intensity-dependent absorbance of the coating. This gives us not only an opportunity to reestablish the mirrors' operation, but also a key for expanding the DM functionality into the nonlinear domain as well as for exploitation of DM as a new kind of nonlinear element suitable for advanced photonic applications.

2. RESULTS

A. Experiment

In our experiments we used intense sub-40-fs laser pulses, carried at central wavelength, λ_L, 400 nm to investigate the reflectance of a series of dispersive DMs, here and further denoted as Mx-series. The light source is an intense *s*-polarized frequency-doubled output from a commercially available chirped pulse two-stage, multi-pass Ti:sapphire amplifier. Second harmonic generation is realized in a thin BBO crystal yielding ~40 fs upchirped pulses at the average power of 3 W at 3 kHz repetition rate. Stepwise attenuation of the light source power can be realized gradually down to 0.5 W without compromising the temporal and spectral characteristics of the pulses by modulating the radio frequency signal power inside the Dazzler [19,20]. With the implementation of the gentle focusing scheme, we were able to gradually adjust the incident peak intensity, I_p, in the range from $\sim 3 \cdot 10^9$ W/cm^2 to $\sim 2 \cdot 10^{12}$ W/cm^2. This intensity range was chosen as it covers the desired working range of the described mirrors, which spans from 10^{10} to 10^{11} W/cm^2. Damage of the tested samples at intensities above 3.5×10^{11} W/cm^2 prevented data collection at higher intensities.

The mirrors of the Mx-series were designed for the wavelength range from 380 to 420 nm, though they differed by the value of the introduced GD ranging from 25 fs (mirror M3) to 100 fs (mirror M2) [Fig. 1(a)]. The mirrors were produced out of a Ta_2O_5/SiO_2 material pair; Ta_2O_5 was used as the high-index material, whereas SiO_2 was the low-index material. Both materials are most commonly used for the production of coatings in the visible (VIS) spectral range, as the band gaps of Ta_2O_5 and SiO_2 deposited by magnetron sputtering are ~4.2 eV [21] and ~7.5 eV [22,23], respectively. Linear absorbance for Ta_2O_5 single layer is estimated to $\sim 0.8 \cdot 10^{-3}$, for $SiO_2 \sim 10^{-4}$. The mirrors were coated on 25 mm diameter, 6.35 mm thick fused silica substrates transparent in the VIS and near-ultraviolet (NUV) spectral ranges by means of magnetron sputtering thin-film deposition technology.

We observed that the DMs had an intensity-dependent reflectance; i.e., the reflectance of the DM decreased with an increase of the incident intensity [Fig. 1(b)]. The observed effect was reversible; i.e., if the incident intensity was decreased, the reflectance instantly rolled back to previously recorded higher values (Fig. 2).

Obtained reflectance curves for the DMs of the series Mx are presented in Fig. 1(b). The plots of Figs. 1(a) and 1(b) show a

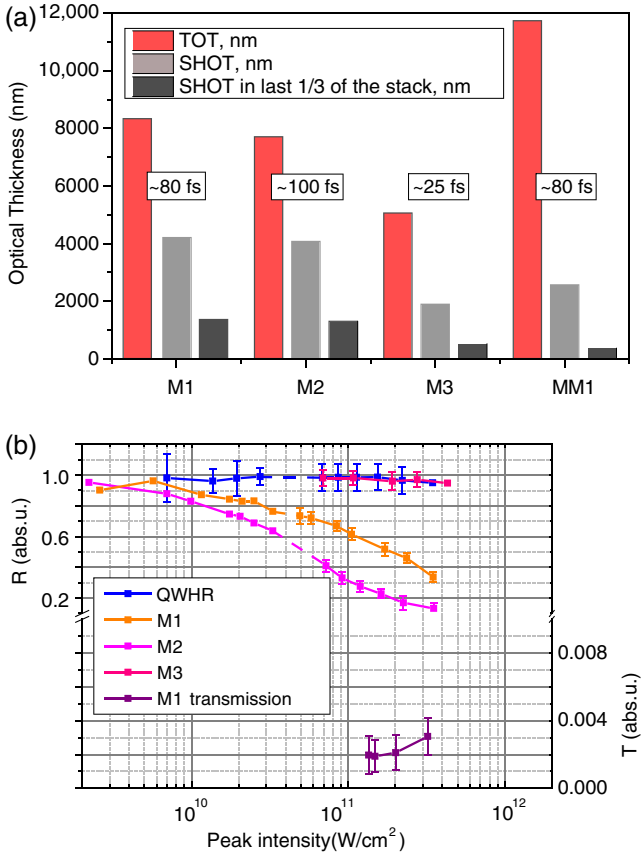

Fig. 1. Intensity-dependent reflectance of the series of nonoptimized DMs. (a) Relevant design data of the tested DMs. Mx refers to nonoptimized DM, MMx-2PA-optimized design. Red bar, total optical thickness of the multilayer stack in nanometers; light gray bar, sum optical thickness of H-index layers in nanometers; dark gray bar, sum optical thickness of H-index layers contained in upper 1/3 of the multilayer stack only. Dispersive properties are represented by the value of introduced GD per reflection (in frame). (b) Nonlinear response of the reflectance of the nonoptimized DM. Solid lines are provided as guidance to the eye. Error bars represent instrumental error of the measurement.

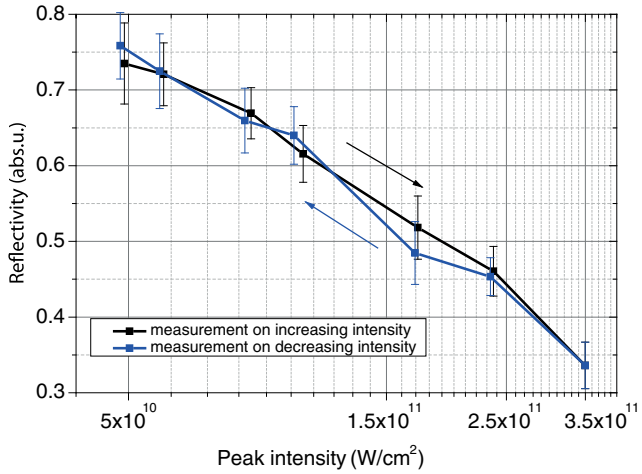

Fig. 2. Reversibility of nonlinear response of the mirror M1. The error bars represent instrumental error of the measurement.

clear dependence of the reflectance on the absolute value of the introduced GD. The smaller the absolute value of introduced GD per reflection, the less pronounced the effect. For instance, the nonlinear response of the mirror M3, introducing the least GD, is significantly weaker than the responses of mirrors M1 and M2, introducing 80 and 100 fs GD, respectively. Furthermore, we tested a quarter-wave high reflector (QWHR) mirror, produced out of the same material pair, that introduces virtually zero dispersion in the spectral range of interest, and did not observe any evidence of nonlinear behavior [Fig. 1(b)].

These observations can be interpreted if one considers the structure of the dielectric mirrors. As most DMs operate on the penetration effect [3] as a basic principle, a certain minimal optical thickness of the coating needs to be reached in order to introduce the desired value of GD [24]. The higher the desired value of GD, the thicker the coating and thus the deeper the electric field penetrates into the multilayer, involving more of the coating material into the interaction. In addition to the penetration effect the presence of resonant cavities [25] creates "hot regions" inside the stack where the electric field is strongly enhanced. Both effects together result in a complicated distribution of electric field within the stack [Fig. 3(a)] that is significantly different from the typical distributions in QWHR or single layers of identical optical thickness [Figs. 3(b) and 3(c)]. Consequently, even relatively small nonlinearities get enhanced and become pronounced in DMs.

In general nonlinearity of optical media can be described by intensity-dependent variations of the complex dielectric constant, or the complex refractive index. In particular, variations of the real part of the complex refractive index are related to Kerr-type nonlinearity. Variations of the imaginary part of the complex refractive index (extinction coefficient) are related to the 2PA and can be described as an increase of the extinction coefficient proportionally to the electric field intensity. The appearance of 2PA absorption causes a noticeable increase of the losses, as the energy is converted to heat, while the optical Kerr effect induces a change of the refractive index and thus modifies the spectral phase. It is illustrated in Fig. 4, representing the group delay dispersion (GDD) characteristic of mirror M1. (For illustration purposes the change in GDD induced by the Kerr effect was simulated using nonlinear refractive index Δn at 800 nm [17].)

We performed thermal tests, where the surface temperature of the irradiated mirrors was directly measured by a thermal camera, and compared the data obtained for the DM M1 and the QWHR produced out of the same materials (Fig. 5). The measurements showed that the surface of the DM warmed up significantly more than that of the QWHR. This significantly verified 2PA to be a leading cause in our experiments.

As 2PA is believed to give the predominant contribution to the appearance of the optical Kerr effect [26], the appearance of strong 2PA should be accompanied by the presence of nonzero nonlinear refractive index n_2. Still the transmittance of the coating has not evidently changed in all the intensity range, staying well within the error of the measurements [Fig. 1(b)]. This observation appears to be rather peculiar. However, the results of [26–28] demonstrate that there is a region in the range of photon energies, E_p, between the direct band gap, E_g, and the 2PA edge, $0.5E_g$, where the nonlinear refractive index is nearly vanishing. This region corresponds to $E_p \sim 0.75E_g$. As the band gap of Ta_2O_5 deposited by the magnetron sputtering technique is an average

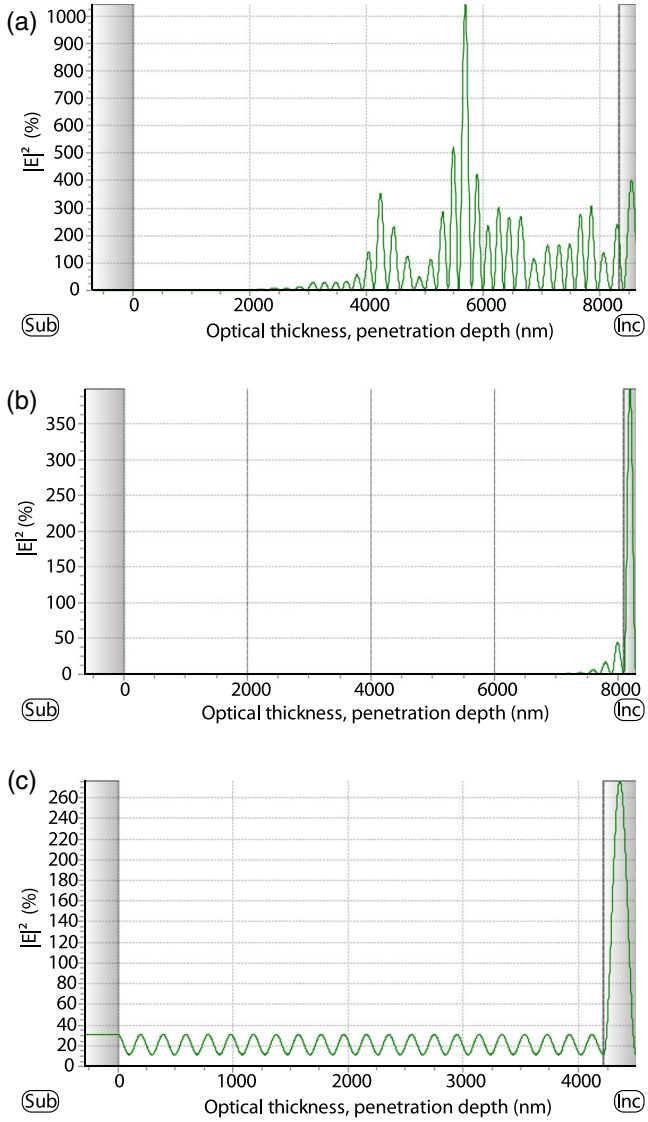

Fig. 3. Electric field distribution at central wavelength of 400 nm, angle of incidence (AOI) = 45 deg, and *s* polarization in different types of the coatings. Values of the electric field are normalized to the amplitude of the incident electric field, E_a. (a) In DM M1. Due to the structure of the DM itself the electric field is enhanced. (b) In quarter-wave high reflector (QWHR). (c) In single layer of high-index coating material of identical optical thickness.

in the range of 4.2 eV and our spectrum covers the region from 380 to 420 nm, E_p in our experiment fits quite well into the predicted range, where the n_2 is nearly vanishing. This fully explains the lack of noticeable changes in n_2.

As we have concluded that the nonlinear refractive index does not experience significant changes, the dispersive properties of the DM should not be affected, only the losses. Thus it is feasible to design a photonic device that demonstrates strong ultrafast nonlinear response to irradiance, while preserving its dispersive characteristics and thus the temporal profile of the reflected pulse. For the realization of the suggested device it is of primary importance to be capable of predicting and possibly tuning the strength of the nonlinear response—in our case, the strength of 2PA. Following the conclusion that 2PA is the main cause of observed nonlinearity, we have developed a model that allows quantitative

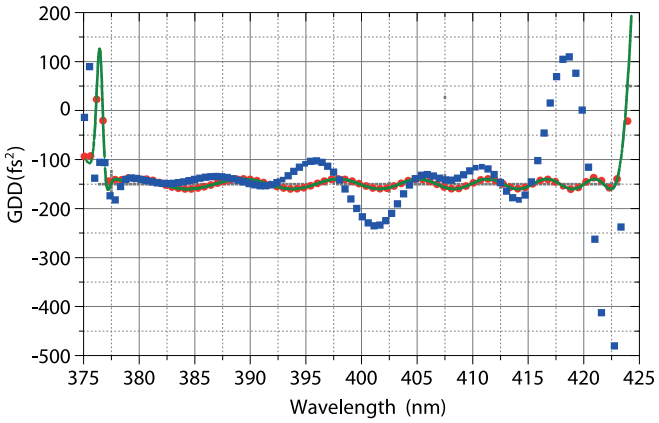

Fig. 4. Impact of different types of nonlinearities on dispersive performance of mirror M1. Green bold line, simulated GDD curve in the range from 380 to 420 nm without impact of either changing nonlinear refractive index or 2PA; red dotted line, simulated GDD curve with the impact of 2PA (estimated spectrally averaged induced absorption is $\Delta\alpha \approx 15.2 \cdot 10^2$ cm^{-1}); blue dotted line, simulated GDD curve with impact of nonlinear refractive index $\Delta n \approx 0.0025$ at corresponding intensity $I_p = (3.5 \pm 0.7) \cdot 10^{11}$ W/cm^2.

and qualitative simulation of the 2PA in thin-film coatings and its subsequent applications.

B. Model

We simulated 2PA in multilayer mirrors as an induced extinction coefficient proportional to the squared electric field amplitude modulus, $\chi(z) = \beta|E(z)|^2$, where z is the coordinate along the mirrors' cross section. Due to the fact that the band gap of SiO_2 is significantly wider than the band gap of Ta_2O_5, we considered an induced extinction coefficient in Ta_2O_5 layers only. While ideally one has to perform this nonlinear interaction step in the time domain, we found that in the case of slowly varying pulses containing ≥30 full optical cycles, the pulses are long enough so that the treatment in the frequency domain can be utilized. Our sub-40-fs pulses centered at 400 nm are ideal for the implementation of such a model. Moreover, consideration in the frequency domain also provides a substantial boost in computational efficiency inheriting successful software packages in the multilayer design [29].

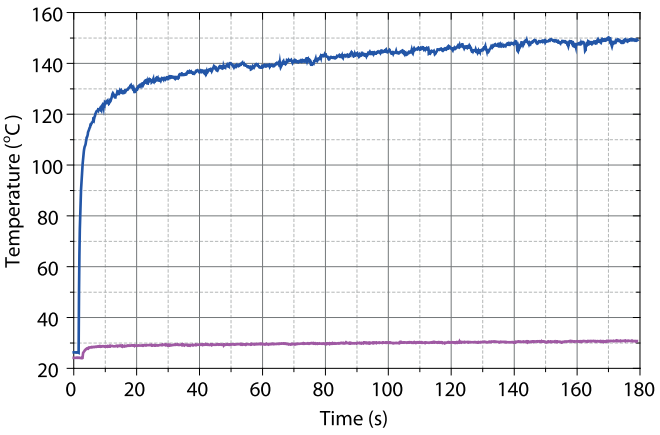

Fig. 5. Thermal tests of nonoptimized designs. Blue bold line, surface temperature of irradiated mirror M1; pink bold line, surface temperature of QWHR. Incident intensity is $I_p = (3.5 \pm 0.7) \cdot 10^{11}$ W/cm^2.

Although the values derived from our implementation, as a consequence of the above consideration, are tightened to our specific laser pulses, the approach to the treatment of 2PA in terms of the induced extinction coefficient, which is suggested here, is universal and can be applied to virtually all possible cases.

Specifically, similar to [30], pp. 4–11, the initial system of Maxwell equations describing the interaction of s-polarized light with the multilayer mirror can be reduced to a boundary-value problem for a system of two nonlinear ordinary differential equations:

$$\frac{du}{dz} = ik\nu, \tag{1a}$$

$$\frac{d\nu}{dz} = ik(\tilde{n}(z,u) - \alpha^2)u, \qquad 0 < z < z_a, \tag{1b}$$

$$\tilde{n}(z,u) = n(z) - i\beta|u(z)|^2, \tag{1c}$$

$$(\nu - q_s u)|_{z=0} = 0, \tag{1d}$$

$$(\nu + q_a u)|_{z=z_a} = 2q_a E_a. \tag{1e}$$

Here $k = 2\pi/\lambda = \omega/c$ is the wavenumber, $u(z)$ and $\nu(z)$ are the tangential amplitudes of the electric and magnetic fields, respectively, and $n(z)$ is the refractive index profile describing the mirror structure. The coordinate $z = 0$ corresponds to the boundary between the coating and the substrate, and the coordinate $z = z_a$ corresponds to the boundary between the coating and the ambient medium. Parameters α and q_s, q_a are defined as $\alpha = n_a \sin\theta$, $q_{s,a} = (n_{s,a}^2 - \alpha^2)^{1/2}$, where n_s and n_a are the refractive indices of the substrate and the ambient medium, θ is the angle of incidence, and E_a is the amplitude of the electric field. The reflectance can be determined as a ratio of the reflected wave intensity to the intensity of the incident wave, which leads to

$$R(k, E_a) = \left| \frac{q_a u(z_a, k) - \nu(z_a, k)}{q_a u(z_a, k) + \nu(z_a, k)} \right|^2. \tag{2}$$

Note that due to the nonlinearity of Eqs. (1) the reflectance is dependent on the incident wave amplitude. Since Eq. (2) is invariant with respect to multiplication of u, ν, and E_a by $\exp(i\phi)$, it is sufficient to study the dependence of $R(k, E_a)$ on the real valued E_a parameter. The dependence of the simulated reflectance Eq. (2) for the mirror M2 versus the intensity of the incident light is shown in Fig. 6 for $\beta = 10^{-6}$. All dependencies are represented with respect to arbitrary intensity. The solid blue curve in Fig. 6 represents the reflectance at the wavelength 400 nm. The reflectance drop is noticeably dependent on the wavelength: the dashed-magenta and the dashed-green curves represent the reflectance at 410 and 390 nm, respectively.

We consider irradiating pulses with spectral distribution having full width at half-maximum (FWHM) of 14 nm around the central wavelength of 400 nm. For relatively long and/or significantly chirped pulses with slowly varying amplitude the model Eqs. (1) and (2) remain valid with sufficient accuracy. In order to take into account the fact that different spectral components of the pulse have different intensities, and as a result have different reflectance due to 2PA nonlinearity, we introduce effective reflectance corresponding to the specified pulse. As the drop of input intensity for wavelengths deviating from the central wavelength of 400 nm obviously leads to a corresponding increase of the reflectance, the effective reflectance is higher than the reflectance at

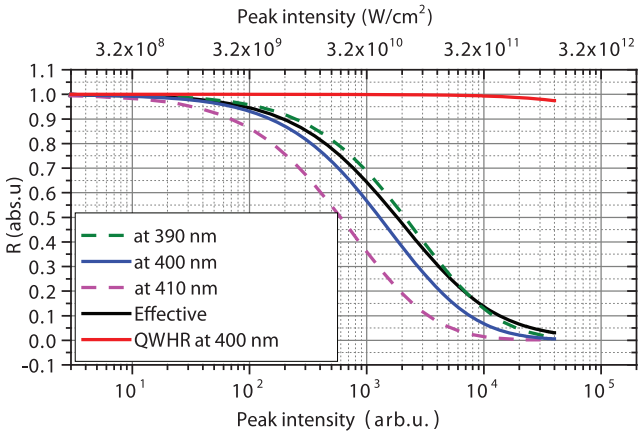

Fig. 6. Simulated intensity-dependent reflectance of the mirror M2 at different wavelengths. Blue, dashed-magenta, and dashed-green curves are reflectance at 400, 410, and 390 nm, respectively. Black curve is the effective reflectance integrated with respect to Gaussian spectrum with the center at 400 nm. For comparison the effective reflectance of a 35-layer quarter-wave mirror with central wavelength of 400 nm is also shown (red curve). Top x scale is relevant peak intensity in SI units calculated via multiplication of peak intensity in arb.u. by $G^2 = (3.2 \pm 0.3) \cdot 10^7$ fitting factor.

the central wavelength, where the intensity of the incident light possesses a maximum value. For simplicity we assumed the spectral distribution of intensity having a Gaussian shape,

$$I_a(k) = \frac{I_0}{\Delta\sqrt{2\pi}} \exp\left(-\frac{(k-k_0)^2}{2\Delta^2}\right), \quad (3)$$

where Δ in Eq. (3) is defined by the FWHM of the pulse spectrum and for $k_0 = 2\pi 25000$ cm^{-1}, corresponding to the central wavelength of 400 nm, is equal to $2\pi 371$ cm^{-1}. The resulting effective reflectance can be obtained as

$$R(I_0) = \frac{1}{\Delta\sqrt{2\pi}} \int R(k, E_a) \exp\left(-\frac{(k-k_0)^2}{2\Delta^2}\right) \mathrm{d}k, \quad (4)$$

where we additionally assumed that E_a is equal to the square root of the dimensionless incident light intensity: $E_a = \sqrt{I_a(k)}$. The black curve in Fig. 6 corresponds to the effective reflectance Eq. (4). Due to the essentially nonlinear origin of the 2PA phenomenon, the effective reflectance does not belong to the area between reflectance curves for 390 and 410 nm. Even more, because of spectral integration the decrease of the reflectance is less pronounced and it occurs at higher values of the incident light intensities compared to monochromatic cases. Note that in Fig. 6 the integrated reflectance is higher than the reflectance at 390, 400, or 410 nm when the arbitrary light intensity is higher than 10^4. For comparison we also presented the effective reflectance of a 35-layer quarter-wave mirror for the central wavelength of 400 nm. This quarter-wave mirror almost does not exhibit any noticeable decrease of the reflectance at the same levels of the incident light. To better illustrate the physical mechanism of the induced extinction coefficient influence on the resulting reflectance values we calculated its profiles for the wavelengths of 390, 400, and 410 nm (Fig. 7). The profile for the wavelength of 400 nm was calculated for the intensity providing 20% reflectance. This intensity is equal to $\approx 4.2 \cdot 10^3$ arb.u. (Fig. 6). Two other profiles for the wavelengths of 390 and 410 nm were calculated for the same intensity level that resulted in reflectance values equal to 0.314 and 0.071, respectively. One can clearly see the correlation between the penetration depth of the induced extinction coefficient and the value of the reflectance.

Since the reflectance $R(k, E_a)$ Eq. (2) is obviously independent with respect to scaling of u and ν by a factor of G and a simultaneous decrease of β by the factor of G^2, the obtained results can help to estimate the value of β by fitting the experimental data. At low intensities mirrors are illuminated with a collimated beam, while at high intensities, where the focusing scheme is implemented, the iris is used to select the most intense part of the beam; therefore it is possible to assume a flat-top spatial distribution across the beam spot. In this case the electric field E_a [V/m] is connected with incident light intensity I [W/cm^2] with the relation $E_a = 10^2\sqrt{2I\eta_0}$, where $\eta_0 \approx 376.7\ \Omega$ is the impedance of vacuum. A good fit of the experimental data related to the mirror M2 is obtained with $G^2 = (3.2 \pm 0.3) \cdot 10^7$ [Fig. 8(a)], and as a result the estimate of β in SI units is $\beta_{si} \approx \beta/(20000\eta_0 G^2) = (4.1 \pm 0.4) \cdot 10^{-21}$ [m^2/V^2]. The obtained value of the 2PA coefficient seems to be rather high; yet the authors were not able to find the 2PA numerical value in the literature. We can compare the 2PA value with other oxides. For this purpose it is necessary to convert the obtained value to one more appropriate for 2PA measurement:

$$\alpha_2 = 8\pi\eta_0\beta_{si}/(n_{Ta_2O_5}\lambda). \quad (5)$$

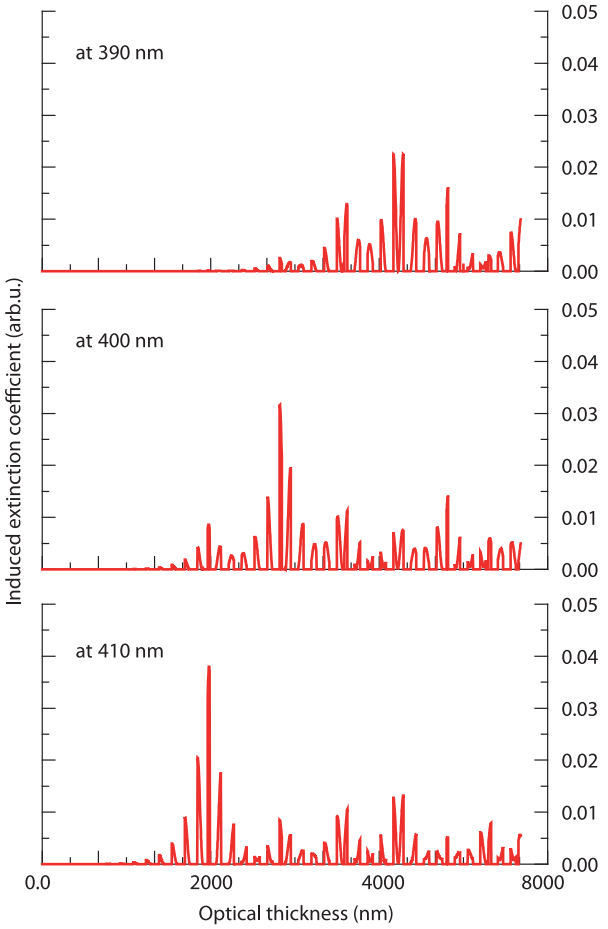

Fig. 7. Distributions of the induced extinction coefficient $\beta|E|^2$ in the mirror M2 cross section for wavelength values: 390, 400, and 410 nm.

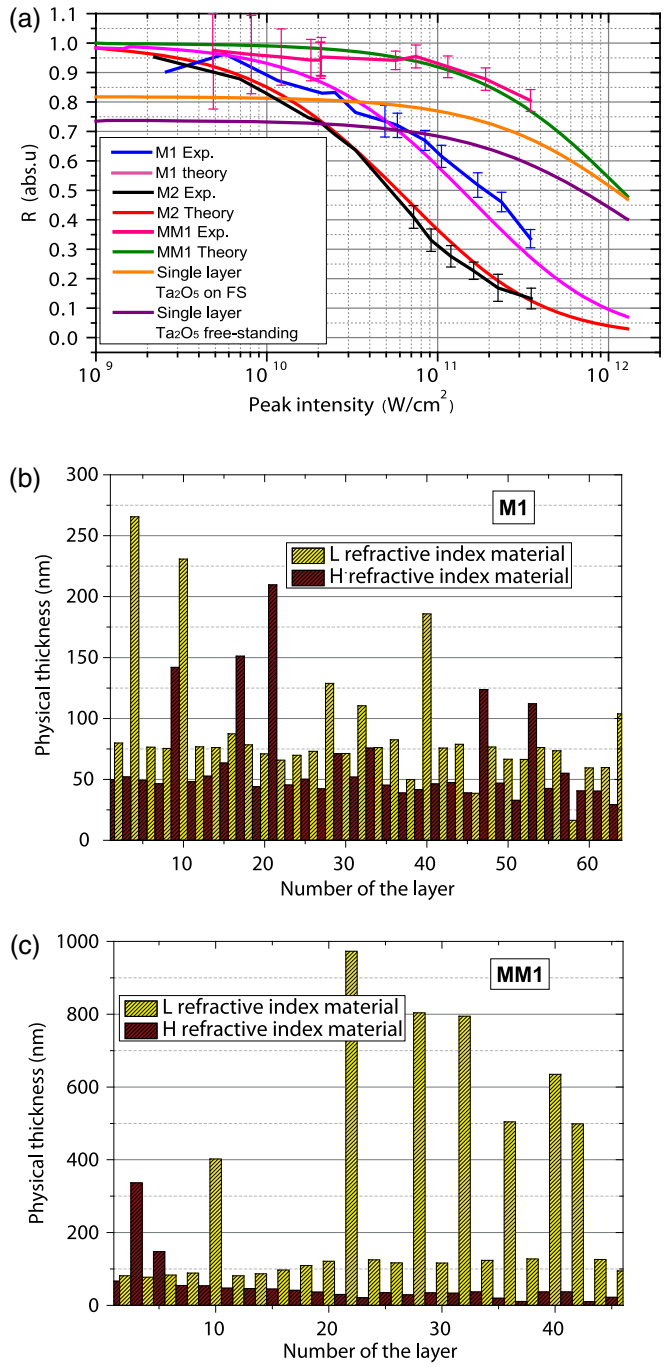

Fig. 8. Optimization of 2PA in dielectric coating. (a) The 2PA parameter β has been estimated by fit of the experimental curve for the mirror M2. Theoretical curves related to the single layer of Ta_2O_5, M1, and MM1 have been calculated with the same 2PA parameter β without additional fitting. Solid lines connecting actual measured data points are provided as a guidance to the eye. Error bars represent the instrumental error of the measurement. (b) Designed stack of nonoptimized M1. The coating contains approximately equal amounts of high-index and low-index material, and the materials are distributed homogeneously. (c) Designed stack of 2PA-optimized MM1. The presence of high-index material is decreased in favor of low-index material, and the high-index material is concentrated farther from the top layers of the stack.

The estimation of the corresponding α_2 value results in $\alpha_2 = (4.35 \pm 0.5) \cdot 10^{-9}$ [cm/W]. It is noticeably higher than similar values for Al_2O_3 ($\approx 0.09 \cdot 10^{-9}$ [cm/W] [31]) measured at 264 nm. On the other hand the corresponding value for TiO_2 is significantly higher [32]: $\alpha_2 = (15/19) \cdot 10^{-9}$ [cm/W]. It is also necessary to take into account that literature data are mainly related to bulk materials, while the optical properties of thin-film materials may significantly differ from the bulk ones. To cross-check the obtained value, we compared the theoretical reflectance of the mirror M1, predicted with the same value of β taken into account, to the experimental data [magenta and blue curves in Fig. 8(a)]. The results demonstrated a convincing correspondence.

In order to confirm that it is the enhancement that plays the major role in the observed nonlinearity, we additionally estimated the theoretical transmittance of a single layer of Ta_2O_5. A single layer has optical thickness equal to the sum the optical thickness of all H-index layers (SHOT) contained in the M2 mirror stack in Fig. 1(a), and is either free standing or deposited on the fused silica substrate, identical to the mirrors' substrates. The obtained curve [Fig. 8(a)] indicates that enhancement of the internal field reached in DM is indeed of major importance, as the reflectance drop of the single layer is significantly less than those simulated and measured for DMs M1 and M2.

3. IMPLICATIONS

The nonlinear absorbance of the coating can be tailored, if along with the coefficient of the linear absorbance, α, the nonlinear extinction coefficient β is taken into account and implemented into the already adopted DM design approaches [33–35]. However, design optimization will require multiple solutions of nonlinear problems and is rather time-consuming for conventional calculations. As a simpler approach, we have estimated the effective induced nonlinear absorption at the highest level of working intensity and introduced linear absorbance of a similar value in high-index layers. This allowed us to develop a new series of 2PA-optimized DMs using conventional multilayer design techniques.

As in this particular case, we were interested in developing a device with dispersion characteristics similar to M1, while achieving the highest possible reflectance, the new 2PA-optimized design targeted minimization of the 2PA. The detailed data of the new mirror, MM1, are summarized in Fig. 1(a). Comparison of the nonoptimized and 2PA-optimized designs reveals major differences. The 2PA-optimized design not only contains less high-index material, but the material is also distributed differently. While in the nonoptimized designs high-index material is distributed homogeneously, with a significant part of it concentrated in the upper layers of the structure where the electric field is strong [Figs. 1(a), 3(a), and 8(b)], in the 2PA-optimized design only a small fraction of high-index material is localized in the upper layers [Figs. 1(a) and 8(c)]. Therefore less of the high-index material is involved into interaction, and, consequently, the influence of the 2PA becomes less pronounced.

Measured reflectance data of the modified design MM1 [Fig. 8(a)] revealed a significant improvement in the performance of the new DM in comparison to mirror M1. Its effective reflectance is higher, and it is less dependent on the incident intensity in the working range of interest. We have also performed transient-grating frequency-resolved optical gating (TG FROG) [36] measurement confirming preservation of the dispersive properties of the MM1 mirror. As the reconstructed pulse duration stayed constant even at the highest incident intensities

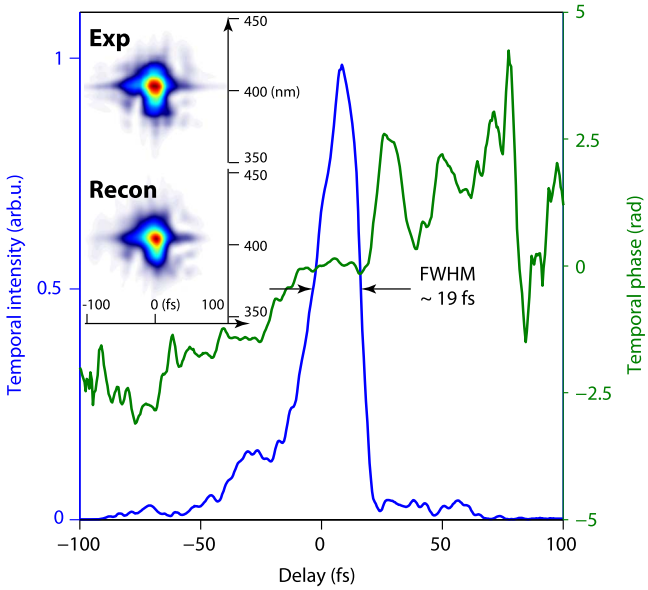

Fig. 9. TG FROG. Reconstruction yields 19 ± 1 fs pulse duration at peak intensities in order of $\sim 10^{11}$ W/cm^2. Inset: actual and reconstructed TG FROG traces.

(Fig. 9), we can conclude that the dispersion properties of the MM1 device are unaffected in all the working range.

The thermal performance has also been verified and also showed noticeable improvement (Fig. 10). The modified design warms up less. Overall, the measured data are in close agreement with the theoretical prediction [Fig. 8(a)], indicating the validity of the developed model and the reliability of the obtained value of β.

4. DISCUSSION

The very strong enhancement of the material nonlinearities in the structure of DM is a novel observation. In general, the third-order nonlinear processes are of high importance for ultrafast optics. The particular manifestation that is of most interest is the optical Kerr effect, which might be used for passive mode locking. Currently, passive mode locking is being realized via implementation of semiconductor saturable absorbers [37–39] or a semiconductor saturable Bragg reflector with single/multiple quantum wells

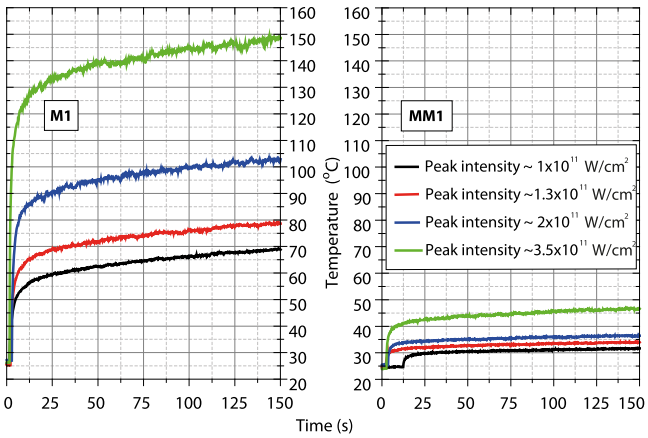

Fig. 10. Thermal tests of 2PA-optimized design.

[40,41]. Unlike saturable-absorber mode locking, passive Kerr-effect mode locking, which is intrinsically not based on saturation effects, should not impose any absorption recovery-time restrictions on minimum pulse duration, thus potentially becoming an attractive alternative for saturable absorbers. Unluckily, advances in this direction are restrained by the mediocre magnitudes on the nonlinear refractive indices of most commonly used materials; thus it becomes challenging to reach the needed reflection modulation depth. There have been attempts to design Kerr-effect-based devices to start passive mode locking, namely in the work of Schirmer and Gaeta [42], but successful experimental realization is yet to be demonstrated. In this respect observed enhancement of the third-order signals might be useful for further advances in this direction.

Meanwhile, the ultrafast [43] character of nonlinear response added to the possibility to strongly enhance the nonlinearity while keeping control on dispersion already opens the potential for implementation of DMs as a new kind of nonlinear element vital for ultrafast applications.

Due to their fast response time, simplicity, compactness, and low cost 2PA absorbers are attractive media for applications in passive all-optical limiting schemes [43] and were successfully exploited in ms to ps laser systems [44,45]. However, when it comes to the ultrafast applications, not only the speed of the limiter, but also its dispersive properties, are becoming a concern, as the appearance of nonlinear phase shift associated with the optical Kerr effect might perturb the temporal–spectral–spatial profile of the ultrafast pulse. Therefore, preservation of the dispersive properties of the limiter during the operation is of major importance. Usage of 2PA DM allows us to circumvent the latter problem, as the mirror preserves its dispersive properties within all the working range.

2PA bulk absorbers are also a typical media for 2PA autocorrelators [46,47] for measurement of UV femtosecond pulses. Unfortunately, they suffer from low signals and dispersion of the active media that puts a restriction on to the minimum measurable pulse duration. Therefore, implementation of 2PA DMs, offering the ability to strongly enhance the nonlinear absorption, potentially improves the signal-to-noise ratio, while simultaneously providing dispersion compensation for the material of the 2PA autocorrelator, thus expanding the capabilities for measuring weak few-femtosecond long pulses [48].

5. CONCLUSIONS

In summary, we have explored the nonlinear response of dielectric DMs. It was found that the cause of the discovered effect is the appearance of third-order nonlinear processes, triggered by very strong enhancement of the internal electric field, which occurs due to the complicated interference in the dispersive multilayer coating. 2PA dominates the response, as the nonlinearity manifests itself in the form of nonlinear absorptance. Despite the strong 2PA, there were no noticeable changes of refractive index of the layer materials, due to correspondence of the E_p to $\sim(0.72/0.74)E_g$, the region where the nonlinear refractive index is in the vicinity of zero. A theoretical model that allows the estimation of the 2PA coefficient and thus prediction and to some extent engineering of the intensity-dependent behavior of any multilayer coating has been developed. In the greater outlook, the observed effect gives a new perspective for the exploitation of third-order nonlinearities for advanced ultrafast photonic applications. In the current state, the ultrafast character of the

explored nonlinearity, the ability to manipulate the strength of the nonlinear response, and the capabilities for dispersion control allow the implementation of DMs as new class of nonlinear components suited for a range of photonic devices. The areas that profit immediately are ultrafast passive all-optical limiting of intense few-cycle laser systems and 2PA autocorrelation measurements of UV femtosecond pulses.

Funding. European Research Council (ERC) (Attoelectronics-258501); European Research Training Network ATTOFEL; Munich Center for Advanced Photonics.

Acknowledgment. We thank C. Wandt for technical support, C. Kealhofer for assistance in styling the text, and I. Angelov and F. Krausz for fruitful discussions.

†These authors had equal contributions to this paper.

REFERENCES

1. U. Keller, "Recent developments in compact ultrafast lasers," Nature **424**, 831–838 (2003).
2. G. Steinmeyer, "Frontiers in ultrashort pulse generation: pushing the limits in linear and nonlinear optics," Science **286**, 1507–1512 (1999).
3. R. Szipöcs, C. Spielmann, F. Krausz, and K. Ferencz, "Chirped multilayer coatings for broadband dispersion control in femtosecond lasers," Opt. Lett. **19**, 201–203 (1994).
4. R. Szipöcs, A. Köházi-Kis, S. Lakó, P. Apai, A. Kovács, G. DeBell, L. Mott, A. Louderback, A. Tikhonravov, and M. Trubetskov, "Negative dispersion mirrors for dispersion control in femtosecond lasers: chirped dielectric mirrors and multi-cavity Gires-Tournois interferometers," Appl. Phys. B **70**, S51–S57 (2000).
5. R. Szipöcs, "Dispersive properties of dielectric laser mirrors and their use in femtosecond pulse lasers," Ph.D. dissertation (SZTE TTK, 2000).
6. V. Pervak, "Recent development and new ideas in the field of dispersive multilayer optics," Appl. Opt. **50**, C55–C61 (2011).
7. T. Brabec and F. Krausz, "Intense few-cycle laser fields: frontiers of nonlinear optics," Rev. Mod. Phys. **72**, 545–591 (2000).
8. C. Manzoni, O. D. Mücke, G. Cirmi, S. Fang, J. Moses, S.-W. Huang, K.-H. Hong, G. Cerullo, and F. X. Kärtner, "Coherent pulse synthesis: towards sub-cycle optical waveforms," Laser Photon. Rev. **9**, 129–171 (2015).
9. H. Fattahi, H. G. Barros, M. Gorjan, T. Nubbemeyer, B. Alsaif, C. Y. Teisset, M. Schultze, S. Prinz, M. Haefner, M. Ueffing, A. Alismail, L. Vámos, A. Schwarz, O. Pronin, J. Brons, X. T. Geng, G. Arisholm, M. Ciappina, V. S. Yakovlev, D.-E. Kim, A. M. Azzeer, N. Karpowicz, D. Sutter, Z. Major, T. Metzger, and F. Krausz, "Third-generation femtosecond technology," Optica **1**, 45–63 (2014).
10. M. Scalora, J. P. Dowling, C. M. Bowden, and M. J. Bloemer, "Optical limiting and switching of ultrashort pulses in nonlinear photonic band gap materials," Phys. Rev. Lett. **73**, 1368–1371 (1994).
11. M. Soljačić and J. D. Joannopoulos, "Enhancement of nonlinear effects using photonic crystals," Nat. Mater. **3**, 211–219 (2004).
12. R. W. Boyd and J. E. Sipe, "Nonlinear optical susceptibilities of layered composite materials," J. Opt. Soc. Am. B **11**, 297–303 (1994).
13. Z.-M. Meng, F. Qin, and Z.-Y. Li, "Ultrafast all-optical switching in one-dimensional semiconductor-polymer hybrid nonlinear photonic crystals with relaxing Kerr nonlinearity," J. Opt. **14**, 065003 (2012).
14. N. Lepeshkin, A. Schweinsberg, G. Piredda, R. Bennink, and R. Boyd, "Enhanced nonlinear optical response of one-dimensional metal-dielectric photonic crystals," Phys. Rev. Lett. **93**, 123902 (2004).
15. G. L. Fischer, R. W. Boyd, R. J. Gehr, S. A. Jenekhe, J. A. Osaheni, J. E. Sipe, and L. A. Weller-Brophy, "Enhanced nonlinear optical response of composite materials," Phys. Rev. Lett. **74**, 1871–1874 (1995).
16. R. Lepkowicz, "Nonlinear photonic crystals for passive switches," SPIE Newsroom, doi: 10.1117/2.1200805.1144 (2008).
17. C.-Y. Tai, J. Wilkinson, N. Perney, C. Netti, F. Cattaneo, C. Finlayson, and J. Baumberg, "Determination of nonlinear refractive index in Ta_2O_5 rib waveguide using self-phase modulation," Opt. Express **12**, 5110–5116 (2004).
18. R. W. Cahn, K. H. Jürgen Buschow, and M. C. Flemings, eds., "Thin-film optical filter," in *Encyclopedia of Materials: Science and Technology* (Elsevier, 2001).
19. P. Tournois, "Acousto-optic programmable dispersive filter for adaptive compensation of group delay time dispersion in laser systems," Opt. Commun. **140**, 245–249 (1997).
20. F. Verluise, V. Laude, Z. Cheng, C. Spielmann, and P. Tournois, "Amplitude and phase control of ultrashort pulses by use of an acousto-optic programmable dispersive filter: pulse compression and shaping," Opt. Lett. **25**, 575–577 (2000).
21. E. Franke, C. L. Trimble, M. J. DeVries, J. A. Woollam, M. Schubert, and F. Frost, "Dielectric function of amorphous tantalum oxide from the far infrared to the deep ultraviolet spectral region measured by spectroscopic ellipsometry," J. Appl. Phys. **88**, 5166–5174 (2000).
22. O. Anderson, "Silicon oxides," in *Thin Films on Glass*, H. Bach and D. Krause, eds. (Springer, 1997), pp. 159–170.
23. H. A. Macleod, "Thin-film optical filters," in *Thin-Film Optical Filter*, E. R. Pike and R. G. W. Brown, eds., 4th ed. (CRC Press, 2010), pp. 5–10.
24. V. Pervak, V. Fedorov, Y. A. Pervak, and M. Trubetskov, "Empirical study of the group delay dispersion achievable with multilayer mirrors," Opt. Express **21**, 18311–18316 (2013).
25. B. Golubovic, R. R. Austin, M. K. Steiner-Shepard, M. K. Reed, S. A. Diddams, D. J. Jones, and A. G. Van Engen, "Double Gires-Tournois interferometer negative-dispersion mirrors for use in tunable mode-locked lasers," Opt. Lett. **25**, 275–277 (2000).
26. M. Sheik-Bahae, D. J. Hagan, and E. W. Van Stryland, "Dispersion and band-gap scaling of the electronic Kerr effect in solids associated with two-photon absorption," Phys. Rev. Lett. **65**, 96–99 (1990).
27. M. Sheik-Bahae, D. C. Hutchings, D. J. Hagan, and E. W. Van Stryland, "Dispersion of bound electronic nonlinear refraction in solids," IEEE J. Quantum Electron. **27**, 1296–1309 (1991).
28. D. C. Hutchings, M. Sheik-Bahae, D. J. Hagan, and E. W. Van Stryland, "Kramers-Krönig relations in nonlinear optics," Opt. Quantum Electron. **24**, 1–30 (1992).
29. A. V. Tikhonravov and M. K. Trubetskov, "Optilayer software," http://optilayer.com.
30. S. F. Furman and A. V. Tikhonravov, *Basics of Optics of Multilayer Systems* (Editions Frontieres, 1992).
31. R. DeSalvo, A. A. Said, D. J. Hagan, E. W. Van Stryland, and M. Sheik-Bahae, "Infrared to ultraviolet measurements of two-photon absorption and n_2 in wide bandgap solids," IEEE J. Quantum Electron. **32**, 1324–1333 (1996).
32. R. L. Sutherland, *Handbook of Nonlinear Optics*, 2nd ed., Vol. **82** of Optical Engineering (Dekker, 2003).
33. A. V. Tikhonravov and M. K. Trubetskov, "Modern design tools and a new paradigm in optical coating design," Appl. Opt. **51**, 7319–7332 (2012).
34. A. V. Tikhonravov, M. K. Trubetskov, and G. W. DeBell, "Application of the needle optimization technique to the design of optical coatings," Appl. Opt. **35**, 5493–5508 (1996).
35. A. V. Tikhonravov, M. K. Trubetskov, and G. W. DeBell, "Optical coating design approaches based on the needle optimization technique," Appl. Opt. **46**, 704–710 (2007).
36. J. N. Sweetser, D. N. Fittinghoff, and R. Trebino, "Transient-grating frequency-resolved optical gating," Opt. Lett. **22**, 519–521 (1997).
37. U. Keller, W. H. Knox, and H. Roskos, "Coupled-cavity resonant passive mode-locked Ti:sapphire laser," Opt. Lett. **15**, 1377–1379 (1990).
38. U. Keller, "Ultrafast all-solid-state laser technology," Appl. Phys. B **58**, 347–363 (1994).
39. U. Keller, K. J. Weingarten, F. X. Kartner, D. Kopf, B. Braun, I. D. Jung, R. Fluck, C. Honninger, N. Matuschek, and J. Aus der Au, "Semiconductor saturable absorber mirrors (SESAM's) for femtosecond to nanosecond pulse generation in solid-state lasers," IEEE J. Sel. Top. Quantum Electron. **2**, 435–453 (1996).
40. S. Tsuda, W. H. Knox, E. A. De Souza, W. Y. Jan, and J. E. Cunningham, "Low-loss intracavity AlAs/AlGaAs saturable Bragg reflector for femtosecond mode locking in solid-state lasers," Opt. Lett. **20**, 1406–1408 (1995).
41. W. H. Loh, D. Atkinson, P. R. Morkel, M. Hopkinson, A. Rivers, A. J. Seeds, and D. N. Payne, "Passively mode-locked Er^{3+} fiber laser using a semiconductor nonlinear mirror," IEEE Photon. Technol. Lett. **5**, 35–37 (1993).

42. R. W. Schirmer and A. L. Gaeta, "Nonlinear mirror based on two-photon absorption," J. Opt. Soc. Am. B **14**, 2865–2868 (1997).
43. D. J. Hagan, "Optical limiting," in *Handbook of Optics*, M. Bass, ed. (McGraw-Hill, 2008).
44. E. W. Van Stryland, M. A. Woodall, H. Vanherzeele, and M. J. Soileau, "Energy band-gap dependence of two-photon absorption," Opt. Lett. **10**, 490–492 (1985).
45. E. W. Van Stryland, Y.-Y. Wu, D. J. Hagan, M. J. Soileau, and K. Mansour, "Optical limiting with semiconductors," J. Opt. Soc. Am. B **5**, 1980–1988 (1988).
46. J. I. Dadap, G. B. Focht, D. H. Reitze, and M. C. Downer, "Two-photon absorption in diamond and its application to ultraviolet femtosecond pulse-width measurement," Opt. Lett. **16**, 499–501 (1991).
47. A. M. Streltsov, J. K. Ranka, and A. L. Gaeta, "Femtosecond ultraviolet autocorrelation measurements based on two-photon conductivity in fused silica," Opt. Lett. **23**, 798–800 (1998).
48. C. Homann, N. Krebs, and E. Riedle, "Convenient pulse length measurement of sub-20-fs pulses down to the deep UV via two-photon absorption in bulk material," Appl. Phys. B **104**, 783–791 (2011).